

CHAPTER THREE

METHODOLOGY

3.1 Synthesis of Ti-MCM-41

All the Ti-MCM-41 materials used in this research are prepared according to the procedure developed by Corma *et al.* [87], which yields MCM-41 material of good quality and reproducibility. Titanium loading of the catalyst is varied by simply changing the amount of titanium source in the synthesis gel. In this way, five Ti-MCM-41 catalysts are prepared whereby the Si/Ti ratios are 25, 55, 66, 80 and 100. The catalyst samples are denoted as 25-TiMCM41, 55-TiMCM41, 66-TiMCM41, 80-TiMCM41 and 100-TiMCM41 respectively.

In this chapter, details on the materials and gases used, methodology of synthesis for the non-silylated Ti-MCM-41 (3.1.1) and silylated Ti-MCM-41 (3.1.2), reaction set-up (3.2.1), catalytic performance and product analysis (3.2.3) are discussed. In addition, the catalysts that show the most promise are further characterized (3.3) using a variety of analysis techniques.

3.1.1 Synthesis of Non-Silylated Ti-MCM-41

(i) Materials

Below are listed the chemical used in synthesis of Ti-MCM-41 (Table 3.1)

Table 3.1: List of Chemical Used in Synthesis of Ti-MCM-41

No.	Chemical	Formula	Brand	Purity(%)
1	Cetyltrimethylammonium Bromide (CTMABr)	$\text{CH}_3(\text{CH}_2)_{15}\text{N}(\text{CH}_3)_3\text{Br}$	Aldrich	-
2	Tetramethylammonium Hydroxide (TMAOH)	$(\text{CH}_3)_4\text{NOH}$	Aldrich	25
3	Titanium Ethoxide (TEOTi)	$\text{Ti}(\text{OC}_2\text{H}_5)_4$	Assay	33
4	Amorphous Silica, Aerosil 200 (SiO_2)	SiO_2	Degussa	-

(ii) Methodology of Catalyst Synthesis

A series of mesoporous titanosilicate Ti-MCM-41 molecular sieves with various Si/Ti ratios, 25, 55, 66, 80 and 100 denoted as 25-TiMCM41, 55-TiMCM41, 66-TiMCM41, 80-TiMCM41 and 100-TiMCM41 respectively have been hydrothermally synthesized at 100^oC for 48 hours, using surfactant like hexadecyl-trimethylammonium bromide as template and tetramethylammonium hydroxide as mineralizer.

An overview of the synthesis procedure is shown in Figure 3.1 and the details are explained below.

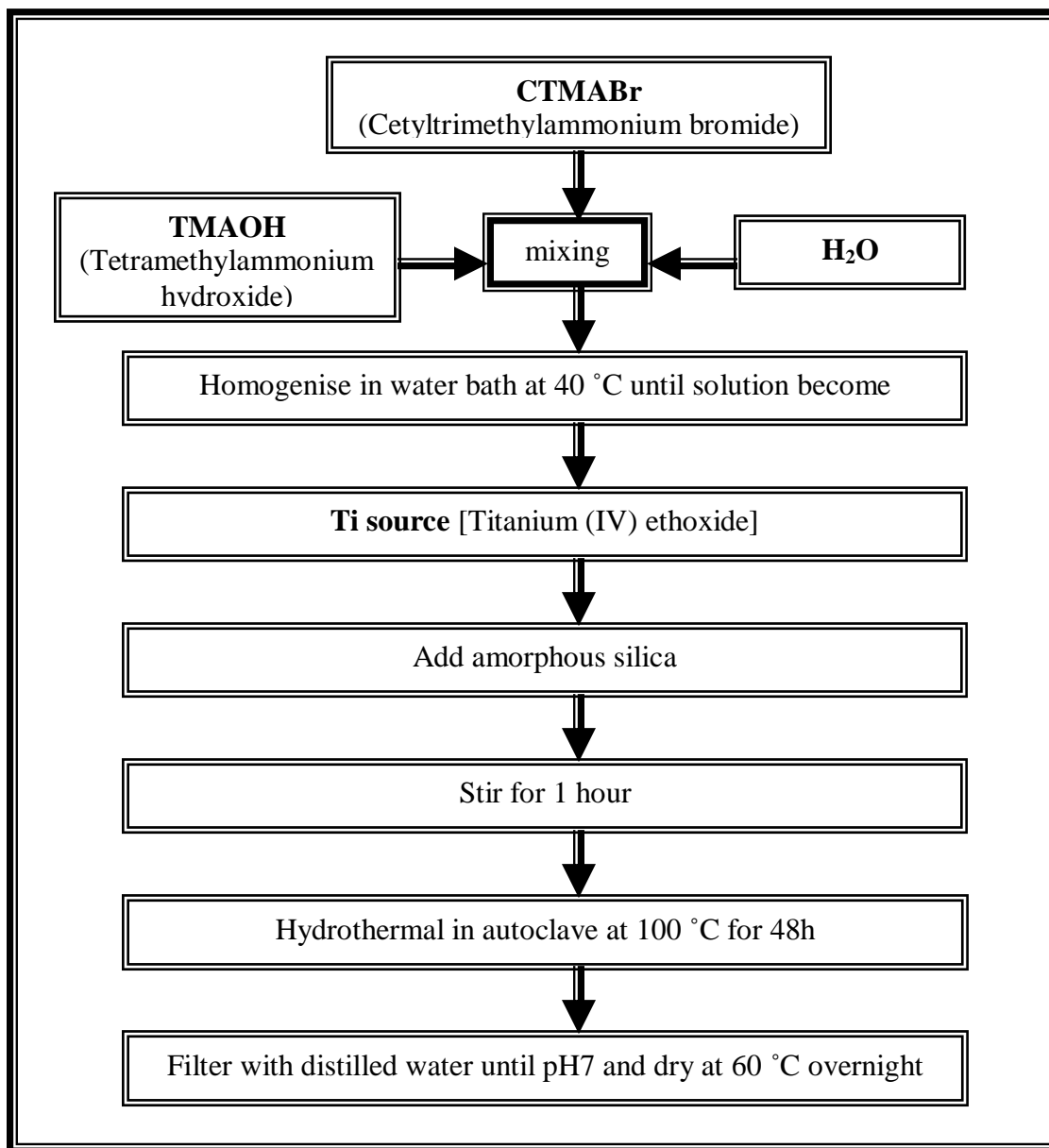


Figure 3.1: Synthesis Procedure of Ti-MCM-41

The procedure is as follows:

An aqueous solution of cetyltrimethylammonium bromide (CTMABr), tetramethylammonium hydroxide (TMAOH) and water are mixed and disorder in water bath until the solution becomes transparent. Then, titanium ethoxide is added and stirred. When the solution is homogenous, silica (SiO_2) is added and stirred for one hour. The molar chemical composition of the synthesis mixtures ($\text{SiO}_2 = 1$) for a given $\text{Si/Ti} = 80$ is;



The molar chemical compositions are similar for each compound in all ratios ($\text{Si/Ti} = 25, 55, 66, 80$ and 100), except for TEOTi, that follows the molar composition as tabulated in Table 3.2.

Table 3.2: Chemical Composition of the Synthesis Mixtures

Compound	Weight (g)		No. of moles	Molecular weight (gmole^{-1})
1) CTMABr	11.39		0.0313	364.1
2) TMAOH	4.9275		0.0541	91.05
3) H_2O (mili-Q)	91.0825		5.0601	18.00
4) TEOTi	Si/Ti	Wt (g)	No. of moles	227.98
	25	1.897	0.0083	
	55	0.862	0.0038	
	66	0.719	0.0032	
	80	0.593	0.0026	
	100	0.474	0.0021	
5) SiO_2	12.5		0.2080	60.09

The gel is then heated in teflon-lined stainless steel autoclaves as shown in Figure 3.2 and 3.3 and crystallization occurs at 100°C for 48 hours.

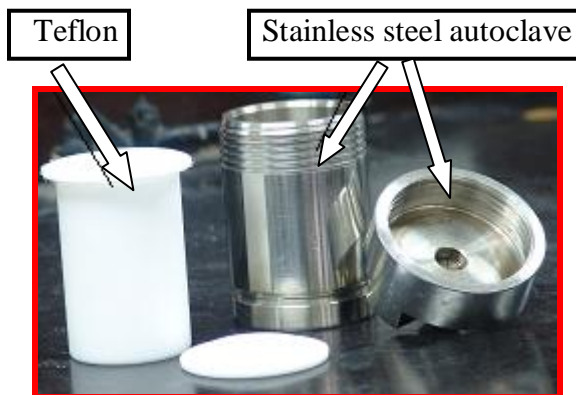


Figure 3.2: Teflon and Stainless Steel Autoclaves



Figure 3.3: Autoclaves Oven

The solid is recovered by filtration and exhaustive washing with distilled water is conducted until neutral pH in the filtrate is obtained. The sample is then dried at 60 °C for 24 hours and calcined.

iii) Calcination Procedure

Before a catalyst can be used efficiently in a reaction, the organic components used as directing agent in crystallization (template) should be burned off. Therefore, calcinations of samples are an important process before a catalytic reaction could take place. Calcination is done in a quartz tubular tube which places the sample, and is connected to a gas system. This quartz tubular tube is covered by a calcination oven, CARBOLITE H-001241 as shown in Figure 3.4.

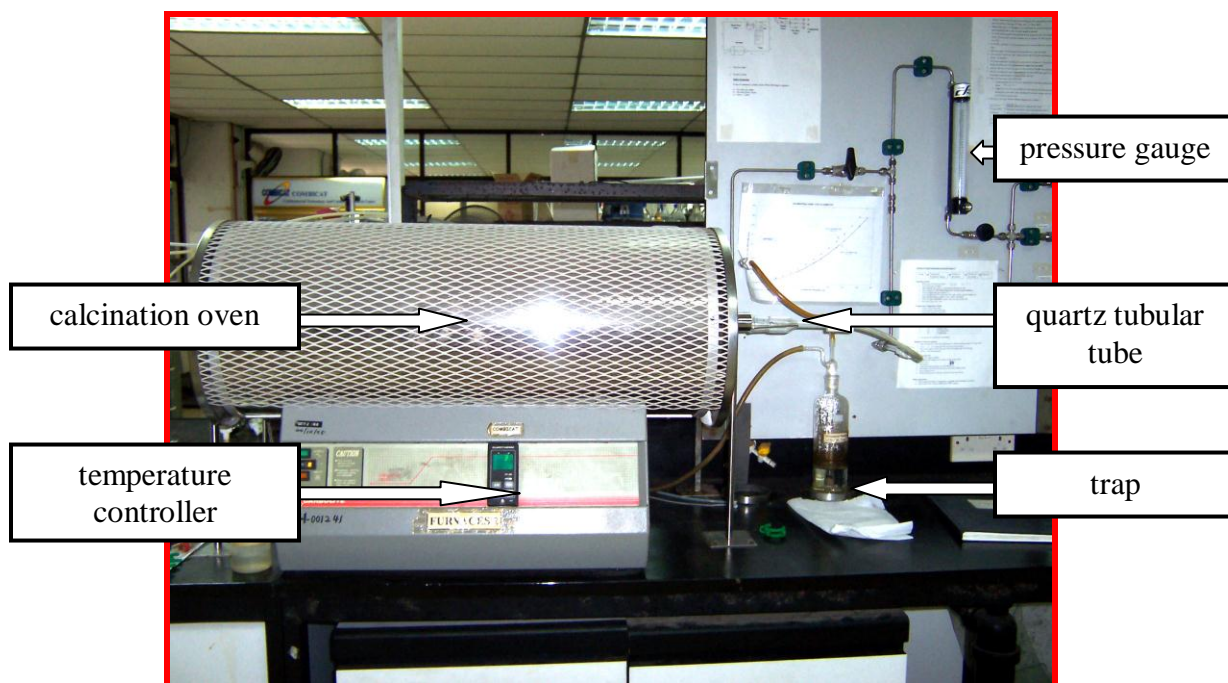


Figure 3.4: Calcination Reactor

For each calcination process, 1 gram of sample is filled in a quartz boat and is placed inside the quartz tubular tube. Two boats of sample are calcined at a time. Calcination is performed using the following conditions: ramp from room

temperature to 540 °C at 3 °C/min in nitrogen atmosphere, hold at 540 °C for an hour, change calcination atmosphere to air, and hold an additional 6 h at 540 °C in air. The programme is shown in Figure 3.5.

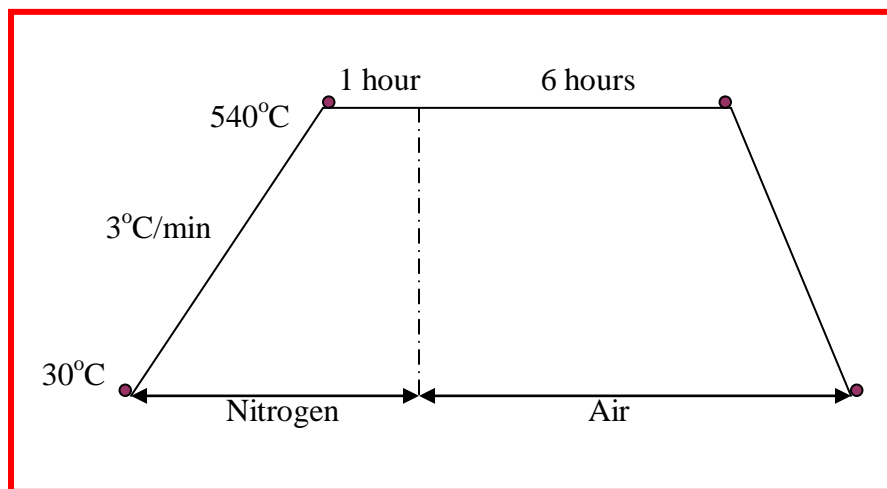


Figure 3.5: Calcination programme for Ti-MCM-41 catalyst

Activation in nitrogen for an hour leads to surfactant decomposition and desorption of organic templates from samples (an endothermic process), in contrast to template burning (an exothermic process) in air. The 6 hours flow in air is also to remove the residual organic compounds. After calcination, a solid sample that has high specific surface area is obtained, hence promote to the better of catalytic activity and selectivity.

3.1.2 Synthesis of Silylated Ti-MCM-41

In this study, the surface property of Ti-MCM-41 is modified by co-condensation of hexamethyldisilazane with the framework of silica source during hydrothermal synthesis. This method allows a high and more controlled loading of organic groups that formed a covalent bond with the inorganic siliceous framework. The strategy is to enhance the hydrophobicity of Ti-MCM-41 materials; at the same time improving their hydrothermal and mechanical stability as well as their catalytic properties.

(i) Materials

Below are listed the additional chemicals used in the synthesis of silylated Ti-MCM-41;

Table 3.3: Additional Chemicals Used in the Synthesis of Silylated Ti-MCM-41

No.	Chemical	Formula	Brand	Purity(%)
1	Hexamethyldisilazane (SiMe ₃)	(CH ₃) ₃ - SiNH - Si - (CH ₃) ₃	Aldrich	97
2	Toluene	C ₆ H ₅ - CH ₃	J. T. Baker	100

(ii) Methodology of Catalyst Synthesis

The preparation of silylated samples involves a similar procedure as in Figure 3.2. After which 1 gram of calcined Ti-MCM-41 is out-gassed at 300°C for 2 hours. Next, 10 grams of solution containing the appropriate amount of hexamethyldisilazane (HMDS) in toluene is added to the dehydrated Ti-MCM-41. The resulting mixture is refluxed under N₂ at 120°C for 2 hours. The silylated sample is then filtrated and washed with 250 ml of toluene. Finally, the sample is dried overnight in an oven at 60°C. The MCM-41 structure is preserved after silylation. Samples with different level of silylation are obtained by changing the HMDS/Ti-MCM-41 (SiMe₃/SiO₂) ratio as shown in Table 3.4.

Table 3.4: SiMe₃/SiO₂ molar ratios employed for Surface Modification of Ti-MCM-41 Catalyst

Sample	(SiMe ₃ / SiO ₂)	Wt. of SiMe ₃ (g)
0.05 Me-TiMCM41	0.05	0.0670
0.20 Me-TiMCM41	0.20	0.2689
0.30 Me-TiMCM41	0.30	0.4019

The SiMe₃/SiO₂ is calculated with the assumption that each hexamethyldisilazane molecule provides two silyl groups (SiMe₃) and the composition of mesoporous Ti-MCM-41 material is SiO₂ (*i.e.* Ti and silanol groups contributions to the final composition are neglected).

The mass of SiMe₃, y required is calculated on the basis of:

- **For SiMe₃ / SiO₂ = 0.05**

$$1 \text{ gm SiO}_2 \longrightarrow 0.01666 \text{ moles SiO}_2$$

$$2 \text{ SiMe}_3/\text{SiO}_2 = 0.05 \longrightarrow \text{moles SiMe}_3 = \frac{0.05 \times 0.01666}{2} = 0.000415$$

$$\text{Wt of SiMe}_3, y = 0.000415 \text{ moles} \times 161.4 \text{ g/mole} = 0.0670 \text{ g}$$

- SiMe₃ / SiO₂ = 0.05
y = 0.0670 g

3.2 Reaction

Catalytic properties of the prepared Ti-MCM-41 with various Si/Ti ratios are determined by means of epoxidation of 1-octene as model compound and pure unsaturated fatty methyl ester: methyl oleate (methyl-9-octadecenoate) as the actual feedstock, using *tert*-butyl hydroperoxide (TBHP) as oxidant. Initially, process optimizations are done on the model compound by highlighting into several parameters; in attempt to achieve the best reaction conditions for methyl oleate. The first parameter to be focused is on the effect of Si/Ti ratio towards catalytic performances of the catalysts, followed by the effect of temperature, alkene:oxidant molar ratio, and reaction time. Based on this optimized conditions, plus the technical, environmental and economical considerations, the heterogeneous catalyzed epoxidation for methyl oleate is further proposed.

3.2.1 Reaction Set-up

Direct heating of reactants usually leads to decomposition rather than reaction and leads to a product that resembles asphalt rather than a clear colorless liquid or pretty white crystal. Furthermore, prolonged heating will simply boil off the solvent. Therefore, there must be some means of returning the solvent vapor back to the reaction flask. This is done by attaching a water-cooled condenser to the reaction flask resulting in a process called heating under reflux.

The basic reflux set-up is shown in Figure 3.6.

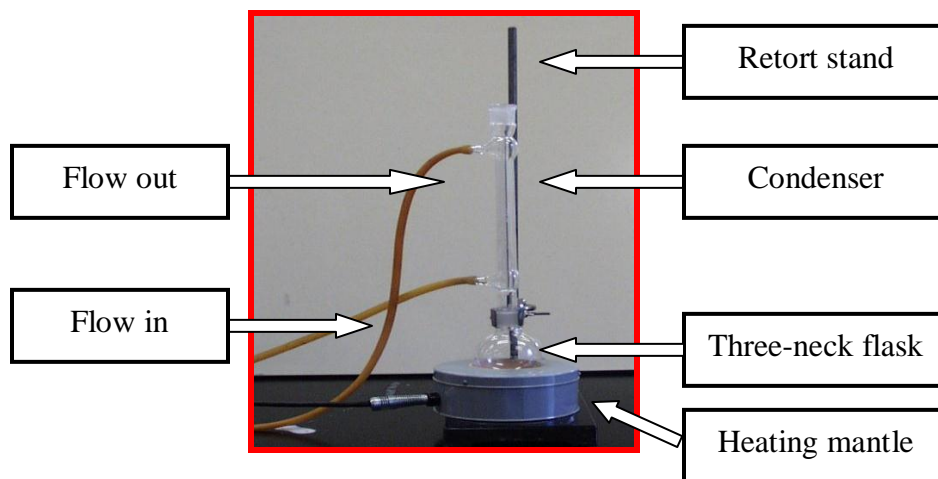


Figure 3.6: Basic Reflux Set-up

In this experiment, the reaction mixture is heated in a “reflux apparatus” consisting of a 25 ml round bottom flask attached to a vertical ethylene glycol-cooled condenser set in a silicon oil bath. The ethylene glycol flows in the bottom of the condenser and out the top.

Ethylene glycol is used rather than water to produce a cooler environment (0–5 °C) in order to avoid discharge of reactant vapor, since 1-octene has a relatively low boiling point. The reflux is for 7 hours long. During reflux, as the reactant boils, the vapor strikes the cooled walls of the condenser, condenses and returns to the reaction flask. Thus, more efficient results are produced.

3.2.2 Materials

Below are listed the chemicals and GC (gas chromatography) standards used in catalytic experiments of Ti-MCM-41;

Table 3.5: List of Chemicals Used in Catalytic Experiment

No.	Chemical	Formula	Brand	Purity (%)
1	1-octene	C_8H_{16}	Fluka	97
2	methyl oleate	$C_{19}H_{36}O_2$	Aldrich	99
3	TBHP	$(CH_3)_3COOH$	Fluka	80

Table 3.6: List of GC Standards Used

No.	Chemical	Formula	Brand	Purity (%)
1	1,2 – epoxyoctane	$C_8H_{16}O$	Aldrich	99
2	1,2 – octanediol	$C_8H_{18}O_2$	Aldrich	99
3	2 – octanone	$C_8H_{16}O$	Aldrich	99
4	1–octen–3–ol	$C_8H_{16}O$	Aldrich	99
5	*Nonane	C_9H_{20}	Aldrich	99

*Internal Standard for GC calibration

3.2.3 Procedure

The epoxidation of 1-octene and methyl oleate with *tert*-butyl hydroperoxide are done in a batch reactor to assess the catalytic performance of Ti-MCM-41 before and after silylation (non-silylated and silylated Ti-MCM-41). The optimization parameters done on model compound are tabulated in Appendix A. In a typical catalytic run, 56 mmole of olefin is mixed with 14 mmole of TBHP (olefin/TBHP = 4) at an optimal reaction temperature of 60^oC for 1-octene and 70^oC for methyl oleate.

The experiments are carried out using an excess amount of olefin as compared to the oxidant, to push the reaction towards product. 0.5 gram of catalyst (6wt% catalyst) is then added to the reaction medium of 1-octene while 0.1 gram (3wt% catalyst) is used for methyl oleate. This instant is taken as time zero of reaction, and aliquots of the reaction media are withdrawn at different reaction times (t=0.5, 1, 2, 4, and 7 hrs).

Subsequently, the samples are analyzed by Gas Chromatography (GC) using a 5% phenyl methyl silicone (HP-5) of 25 meters length column for 1-octene, and 5% phenyl polycarbonate-siloxane (HT-5) of 12 meters length for methyl oleate. Nonane (Aldrich, 99%) is used as internal standard for both feedstocks. The GC temperature programmed is optimized (to obtain good compound separation) in accordance to the samples component and is given in Appendix B. Retention times of products and reactants are shown in Appendix C.

Figure 3.7 shows an overview on the experimental procedure of epoxidation reaction.

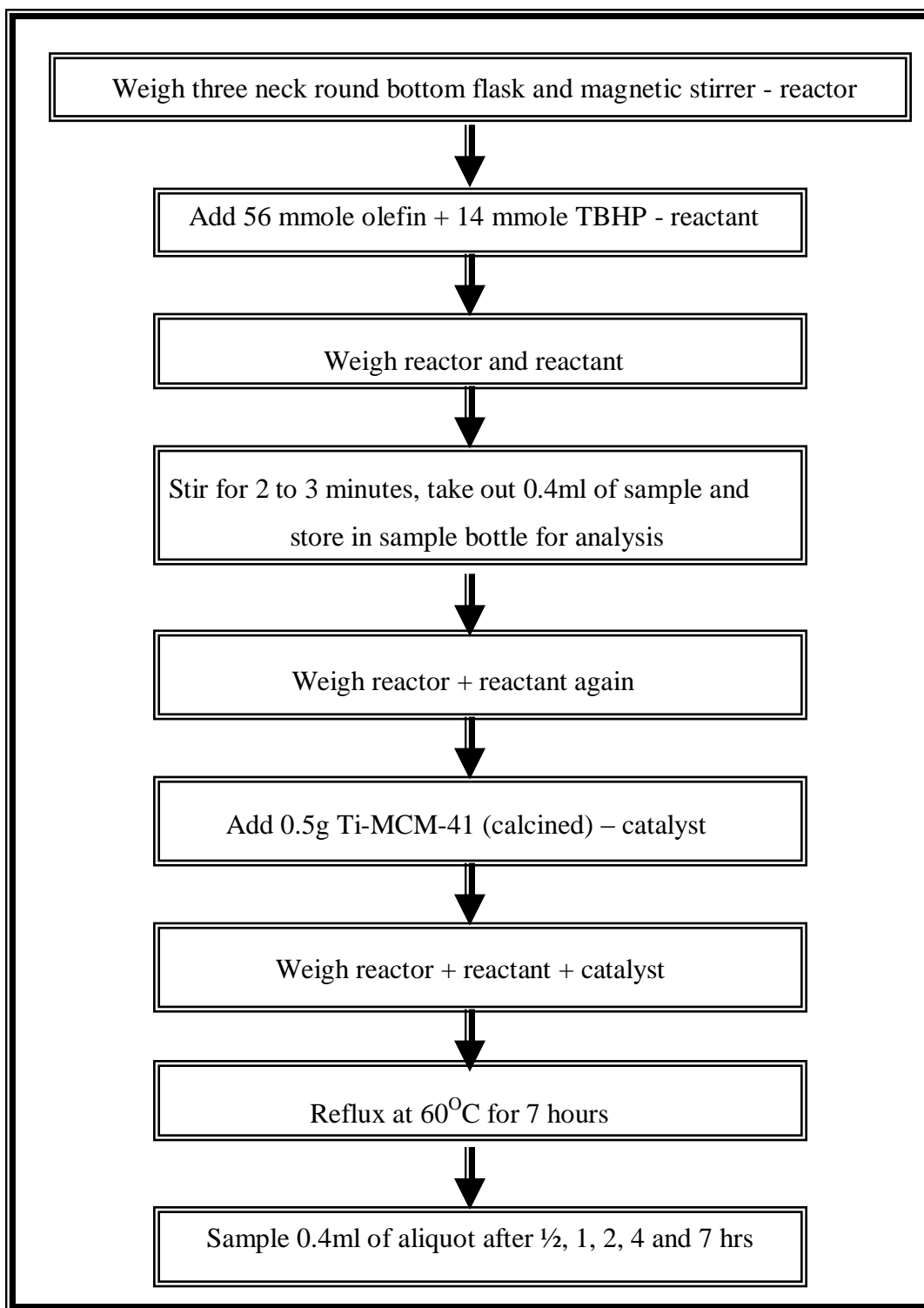


Figure 3.7: Catalytic Experiments of Ti-MCM-41

(i) Analysis of reaction mixtures

Reaction mixtures are analyzed by gas chromatography-mass spectrometry (GC-MS).

(ii) Activity calculation

For the conversion (X) of alkene (1-octene, methyl oleate), the following definition is used;

$$\mathbf{X (\%)} = \frac{\mathbf{\% \text{ of mole of products}}}{\mathbf{\text{conversion maximum (\%)} [\text{from chromatogram}]}} * \mathbf{100\%}$$

where

$$\text{i) \% of mole of products} = \frac{\text{total mole of products}}{\text{total mole of starting material}} * 100$$

$$\text{ii) conversion maximum (\%)} = \frac{\text{mole of initial oxidant}}{\text{mole of initial starting material}} * 100$$

The selectivity (S) to epoxide is defined as follows;

$$\mathbf{S (\%)} = \frac{\mathbf{\text{total mole of epoxide produced}}}{\mathbf{\text{total mole of products}}} * \mathbf{100\%}$$

Another set of calculation, expressed as turnover number (TON) was carried out to determine the productivity of catalyst. Defined as total moles of product produced per one mole of catalyst, the formula is shown below;

$$\mathbf{TON} = \frac{\mathbf{\text{total mole of epoxide produced}}}{\mathbf{\text{weight of catalyst (g)} * \% \text{ of TiO}_2}} * \mathbf{MW \text{ of TiO}_2}$$

3.3 Characterization Techniques

This section discusses the type of characterization methods done to understand the thermal and chemical composition, structural and morphology and also catalytic properties of MCM-41 group catalysts, developed in this work. On one side, this information is essential for deriving relations between their chemical and physicochemical properties and on the other, is for sorptive and catalytic properties.

The physical measurement characterizes the mesoporous structure of the material while chemical measurement determines the silica structures and active sites. There are three independent techniques for the physical measurement: N₂ sorption (adsorption and desorption) analysis, X-ray diffraction (XRD) and Scanning Electron Microscope and Energy Dispersive X-ray Analysis (SEM/EDX).

The chemistry of silica structure and active sites are determined using diffuse reflectance UV-visible spectroscopy (UV-vis) and Fourier Transform Infrared (FTIR). Thermal properties are measured using Thermal-Gravimetric (TGA) and differential scanning calorimetric (DSC) analysis.

Typical analytical approaches and the probed chemical or structural information are summarized in Table 3.7.

Table 3.7: Compilation of characterization techniques

Technique	Synonym	Structure	Pore size	Chemical composition	Functional groups
Electron microscopy	SEM/EDX	•	•	•	
Sorption of probe molecules			•		•
Thermogravimetry, Differential scanning calorimetry	TGA/DSC		•	•	•
Vibrational spectroscopy	FTIR	•	•	•	•
X-Ray diffraction	XRD	•		•	
Model reaction			•	•	•

The principal interest of Ti-MCM-41 materials resides in its potential as oxidation catalyst. The isomorphous substitution and therefore, the incorporation of titanium in the silica framework are not easy to ascertain, and hence, a combination of several techniques is required to provide the necessary information. Several characterization tools have been developed in order to confirm the presence and the amount of titanium (IV) framework sites, as reported in Table 3.8.

Table 3.8: Characterization methods applied to confirm the presence of framework

Ti(IV)

Technique	Expected information	References
XRD	*Phase purity and crystallinity *Quantification of titanium framework by linear regression between unit cell parameters and amount of titanium in the framework *To the different equations proposed, can be attributed to the different amount of titanium reported, while no significant differences have been reported for the higher cell parameters	[88, 89]
FTIR	*Presence of a band at about 960 cm^{-1} attributed to framework of titanium	[88]
UV-vis	*The band in the range 190-210 nm is attributed to charge transfer of titanium (Td) sites, while segregated octahedral TiO_2 absorbs at 310-330 nm	[90]

The basic concepts of each characterization techniques as well as the instruments used are briefly discussed.

3.3.1 Nitrogen Physisorption (BET)

Nitrogen physisorption probes the textural properties of materials, *i.e.* specific surface area, pore volume, pore size (distribution), pore geometry and pore shape.

Brunauer-Emmet-Teller (BET) method is the most widely used standard

procedure for the determination of surface area of finely divided and porous material.

Pores can be varied in size and shape from one adsorbent (adsorbed molecule) to another. Depending on the shape of either cylindrical pores or slit pores, pore size is expressed in terms of diameter or width. Pores with diameters or widths of less than 20 Å are micropores. Intermediate pores between 20 Å and 500 Å are mesopores, and macropores are the pores with openings exceeding 500 Å [91]. Nitrogen physisorption at -196 °C is currently used to determine the specific surface area of an adsorbent and to characterize the micro-, meso- and / or macropores (BET method, t-plot analysis, and capillary condensation).

Figure 3.8 shows nitrogen physisorption instrument for structure and composition measurements.

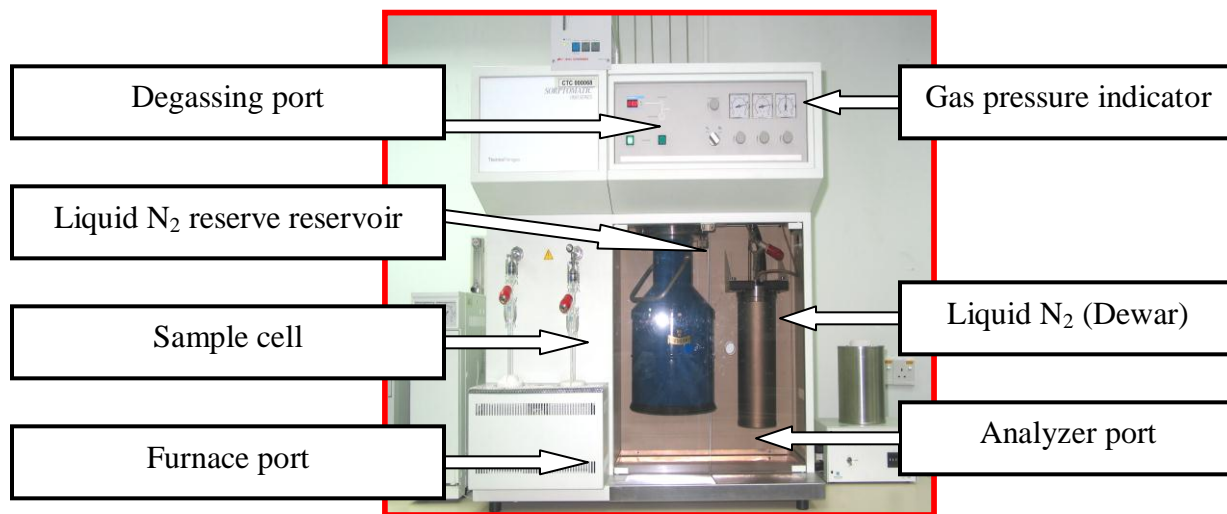


Figure 3.8: Nitrogen physisorption instrument

The BET method is based on a kinetic model of the adsorption process by Langmuir in which the surface of the solid was regarded as an array of adsorption sites. A dynamic equilibrium was assumed between the rate of molecules condensing from gas phase onto the bare sites and the rate at which molecules evaporate from occupied sites. The two rates are equal at that stage.

To determine the characteristics of the adsorbent (adsorbed molecule), the adsorption and desorption isotherms must be established. The isotherm is the standard volume adsorbed as the function of relative pressure. Relative pressure is defined as the ratio of actual gas pressure over the saturated vapour pressure of

adsorbate (P_0), under constant temperature (liquid nitrogen temperature at atmospheric pressure).

The famous BET equation applicable at low P/P_0 range is customarily written in linear form;

$$\frac{P}{v_a(P-P_0)} = \frac{1}{V_m * C} + \frac{(C-1)P}{V_m * C * P_0}$$

where v_a is the number of moles adsorbed at the relative pressure P/P_0 , V_m is the monolayer capacity and C is the so-called BET constant, which according to the BET theory, is related to the enthalpy of adsorption in the first adsorbed layer and gives information about the magnitude of adsorbent-adsorbate interaction energy [92].

If the information is applicable, a plot of $p/[v_a(P/P_0)]$ vs. P/P_0 should yield a straight line with intercept $1/V_m C$ and slope $(C-1)/V_m C$. The value of V_m and C may then be obtained from a plot of a single line, or regression line through the points [93].

IUPAC conventions have been proposed for classifying pore sizes and gas sorption isotherms that reflect the relationship between porosity and sorption. According to IUPAC [94, 95], adsorption isotherms can be classified in six types as illustrated in Figure 3.9, *i.e.*, microporous (type I), nonporous or macroporous (types II, III, and VI) or mesoporous (types IV and V) [96].

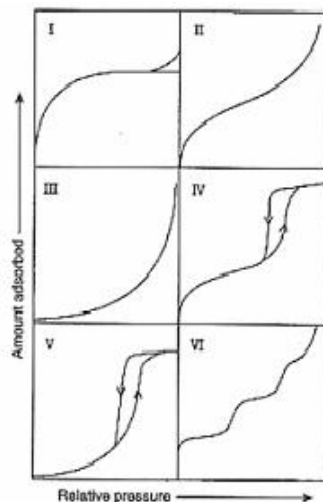


Figure 3.9: The IUPAC classification of adsorption isotherms [97].

The type I is a Langmuir isotherm with very small pores or microporous adsorbent/ solids and chemisorption isotherms. The adsorbate uptake rate depends on the accessible microprobe volume instead of the internal surface area at which adsorption occurs by filling micropores in order of increasing size. Type II is shown by finely divided nonporous solids. Type III and Type V are typical of vapors, *i.e.*, water on hydrophobic solids.

Type IV and Type V feature a hysteresis loop generated by capillary condensation in mesopores. Sometimes, the hysteresis loop is presented at the near saturation pressure region due to presence of mesopores with an upper size restriction [98]. The rare Type VI, the steps like-isotherm, is the isotherm of a nonporous solid associated with layer by layer adsorption on a highly uniform surface. The step's sharpness is dependent on the system and the temperature.

Experimental Conditions:

BET specific surface areas, pore sizes and pore size distribution for the materials used and total pore volume were determined from N₂ adsorption-desorption isotherm obtained using a classical BET volumetric apparatus. The N₂ adsorption-desorption was performed by using Micromeritic Tristar Surface Area and Porosity Analyzer Instrument. The samples (500mg) were loaded into the sample tube and then covered with a seal frit. The sample tube were loaded into the degassing port and out-gassed under flowing of nitrogen at 400°C in vacuum. The sample was left overnight to allow the pressure reaching 40 µmHg. The mass of the sample after degassing was then recorded, and the sample tube mounted on analysis port.

The sample was then immersed in liquid nitrogen and evacuated to 20 µmHg, at which point the dosing gas changed from helium to nitrogen, in the analysis manifold. The isotherm of nitrogen adsorption is measured at liquid nitrogen temperature (-196°C). The specific surface areas were calculated using the BET equation based on the adsorption data in the relative pressure P/P₀ range between 0.0 and 1.0. The pore distribution analysis was based on the method of Barrett-Joyner-Halenda (BJH) applied on the desorption branch of the isotherms.

3.3.2 X-Ray Powder Diffraction (XRD) Analysis

Powder X-ray Diffraction (XRD) is one of the primary techniques used by solid state chemistry for structural and chemical characterization of crystalline materials such as phase identification, phase composition, phase concentration and crystallite size. XRD has been used in two main areas, for the fingerprint of crystalline materials and the determination of their structure. Each crystalline solid has its unique characteristic X-ray powder pattern which may be used as a 'fingerprint' for its identification. One can also determine the size and shape of the unit cell for any crystalline compound using the diffraction of X-rays. The information contained in powder diffractogram is listed in Table 3.9.

Table 3.9: Information contained in the powder diffractogram

Feature	Information
Peak position (2θ value)	Unit Cell Dimension
Non-indexable Line	Presence of Crystalline impurities
Background	Presence of amorphous material
Width of Peak	Crystalline Size
Peak Intensities	Crystal Structure

The X-ray Diffraction instrument consists of an X-ray source, sample holder, and detector as illustrated in Figure 3.10. The diffractometer can be in different configurations *e.g.* theta/theta or theta/2theta.

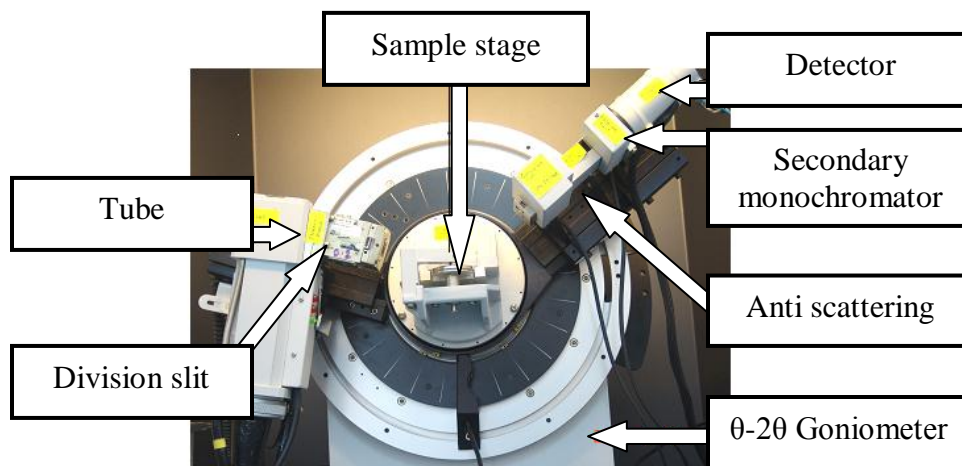


Figure 3.10: X-ray Diffraction

As the name suggests, the sample is normally in a powder form. This really means that the crystalline domains are randomly oriented in the sample. Therefore, when a 2-D diffraction pattern is recorded, it shows concentric rings of scattering peaks corresponding to the various d-spacing in the crystal lattice (d_{hkl}). The positions and the intensities of the peaks are used for identifying the phase of the material. For example, the diffraction lines of graphite would be different from diamond even though they both are made of carbon atoms.

d_{hkl} for a relatively big crystal can be obtained by using the idea of Bragg's law as illustrated in Figure 3.11.

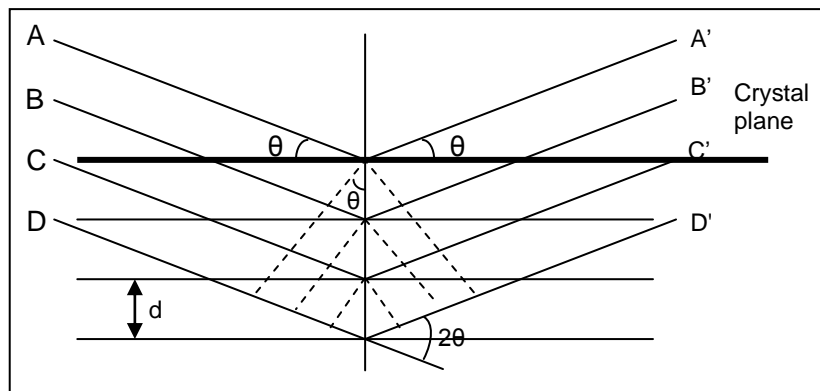


Figure 3.11: Bragg reflection of X-rays from parallel planes of atoms [99].

For constructive interference to occur, the emerging beams A', B', C', D', from crystal plane regenerates a plane wave front corresponding to the incident wave front ABCD. The ray BB' that strikes the second plane travels further than the ray AA', and the ray CC' goes further still. The extra distance travelled by BB' relative to AA' is $2d \sin \theta$, where d is the interplanar distance and θ is the angle of incidence.

Bragg expressed this in an equation now known as Bragg's law:

$$2d \sin \theta = n\lambda$$

θ is the angle between the incident rays and the surface of the crystal

d is the spacing between two layers of atoms

λ is the wavelength of the rays, n is an integer.

The integer n tells us the number of 'extra' wavelengths travelled by BB', or the number of cycles that BB' is retarded relative to AA' and n is called the order of the reflection. Reflection with $n = 2, 3, \text{etc.}$ are called second order, third order, and so on. It follows that a bright reflection should be observed when the glancing angle satisfies the Bragg's Law.

Experimental Conditions:

X-ray diffraction (XRD) analyses were carried out to identify the crystal lattice dimensions, structure and composition of material using a Philips automated PW 1877 equipped with an X'Pert Data Collector for data acquisition and analysis. Data were acquired using a $\text{CuK}\alpha$ monochromated radiation source operated at 40 kV and 40mA at ambient temperature. The material under test was carefully ground to a fine powder and placed evenly on a plastic holder with a dent of 1 inch in diameter and 1/10 inch in depth. Next, it was pressed using a quartz plate to pack the material onto the holder until it was flattened. The excess was scraped off using a razor blade to give an even surface.

The sample holder was then placed in the diffractometer stage for analysis. A divergence slit was inserted to ensure the x-rays focus only the sample and not the edges of the specimen holder. The diffracted/scattered beam passes through the secondary monochromator and is collected by a scintillation detector. The intensity data were recorded by continuous scan in a 2θ mode from $1.0\text{-}20.0^\circ$ with

a step size of 0.03° and 5.00 s counting time each step. The X-ray diffraction pattern is collected at a rotation speed of $0.006^\circ/\text{s}$, in order to obtain a good signal to noise ratio.

3.3.3 Scanning Electron Microscopy (SEM) and Energy Dispersive X-ray Analysis (EDX) Analysis SEM/EDX

As mentioned in section 3.3.1, BET is known to be the method to determine the specific surface area. However, this piece of information leads more to the way the particles are formed rather than to reveal the breadth of particle sizes accurately. Therefore, the best way to observe the particle size distribution is by Transmission Electron Microscopy (TEM). This method possesses the capability to characterize not only the imaging of microstructure directly, but also the identification of the phases presents in a specimen, which leads to a very high cost instrumentation. Nevertheless, the second best method available that is used in this study is by Scanning Electron Microscopy (SEM/EDX). Figure 3.12 shows the SEM/EDX equipment.

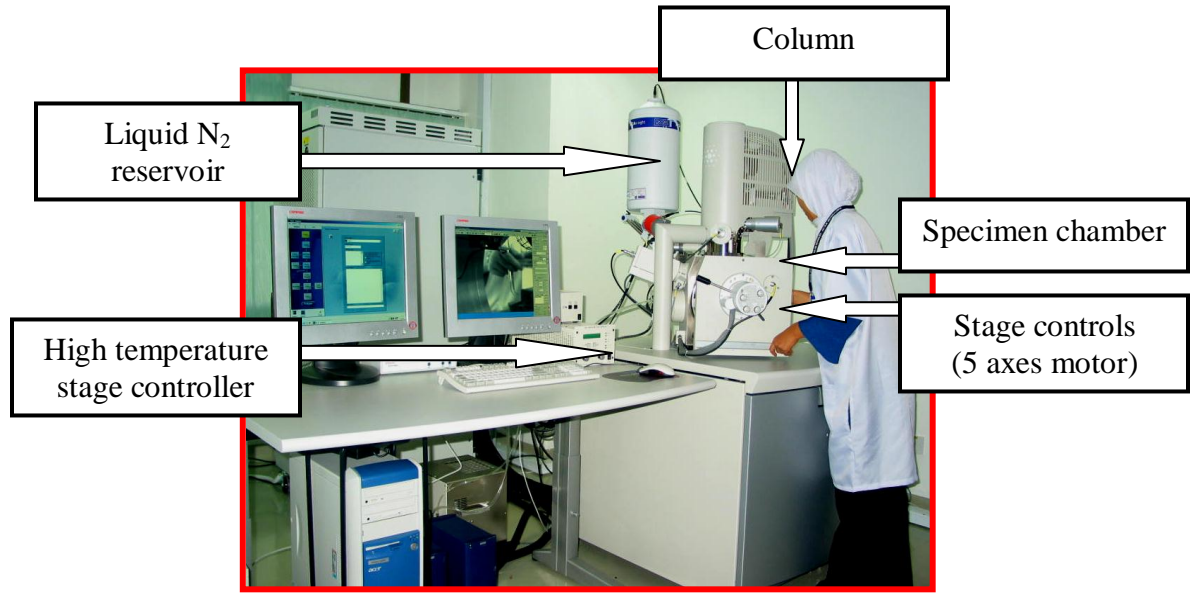


Figure 3.12: SEM/EDX to determine material morphology, surface elemental composition, elemental mapping and in-situ experimentation

SEM produces images of the morphology of particles and surface topology of the crystalline materials. It is also used for inspecting topographies of specimens at a very high magnification, which can go up to more than 300,000 X; but most semiconductor manufacturing applications require magnifications of less than 3,000 X only. SEM inspection is often used in the analysis of die/package cracks and fracture surfaces, bond failures, and physical defects on the die or package surface [100, 101].

During SEM inspection, a beam of electrons is focused on a spot volume of the specimen, resulting in the transfer of energy to the spot. These bombarding electrons, also referred to as primary electrons, dislodge electrons from the specimen itself. The dislodge electrons, also known as secondary electrons, are

attracted and collected by a positively biased grid or detector, and then translated into a signal.

To produce the SEM image, the electron beam is swept across the area being inspected, producing many such signals. These signals are then amplified, analyzed and translated into images of the topography being inspected. Finally, the image is shown on a CRT.

The energy of the primary electrons determines the quantity of secondary electrons collected during inspection. The emission of secondary electrons from the specimen increases as the energy of the primary electron beam increases, until a certain limit is reached. Beyond this limit, the collected secondary electrons diminish as the energy of the primary beam is increased, because the primary beam is already activating electrons deep below the surface of the specimen. Electrons coming from such depths usually recombine before reaching the surface for emission.

Besides secondary electrons, the primary electron beam results in the emission of backscattered (or reflected) electrons from the specimen. Backscattered electrons possess more energy than secondary electrons, and have a definite direction. As such, a secondary electron detector cannot collect them, unless the detector is directly in their path of travel. All emissions above 50 eV are considered to be backscattered electrons.

A SEM that equipped with an EDX analysis system as used in this study enables it to perform compositional analysis on specimens. EDX analysis is useful in identifying materials and contaminants, as well as estimating their relative concentrations on the surface of the specimen.

EDX Analysis stands for Energy Dispersive X-ray analysis and sometimes is referred to as EDS or EDAX analysis. It is a technique used for identifying the elemental composition of the specimen, or an area of interest thereof. During EDX analysis, the specimen is bombarded with an electron beam. The bombarding electrons collide with the specimen atoms own electrons, knocking some of them off in the process. A higher-energy electron from an outer shell eventually occupies a position vacated by an ejected inner shell electron. To be able to do so, however, the transferring outer electron must give up some of its energy by emitting an X-ray.

The amount of energy released by the transferring electron depends on which shell it is transferring from, as well as which shell it is transferring to. Furthermore, the atom of every element releases X-rays with unique amounts of energy during the transferring process. Thus, by measuring the amounts of energy present in the X-rays being released by a specimen during electron beam bombardment, the identity of the atom from which the X-ray was emitted can be established.

The output of an EDX analysis is an EDX spectrum. The EDX spectrum is just a plot of how frequently an X-ray is received for each energy level. An EDX spectrum normally displays peaks corresponding to the energy levels for which the most X-rays had been received. Each of these peaks is unique to an atom, and therefore corresponds to a single element. The higher a peak in a spectrum, the more concentrated the element is in the specimen.

An EDX spectrum plot not only identifies the element corresponding to each of its peaks, but the type of X-ray to which it corresponds as well. For example, a peak corresponding to the amount of energy possessed by X-rays emitted by an electron in the L-shell going down to the K-shell is identified as a K-Alpha peak. The peak corresponding to X-rays emitted by M-shell electrons going to the K-shell is identified as a K-Beta peak.

Experimental Conditions:

Scanning electron micrographs of the samples were taken on a scanning electron microscope (SEM) Philips, Quanta FEG 200 model, equipped with an EDX spectrometer from Oxford instruments. XT microscope software was used for data acquisition and analysis.

The samples were deposited in an aluminum stub using carbon conductive tape. The stub was then mounted on a holder and loaded into the chamber. The following operational parameters were applied:

Accelerating voltage	: HV 5 kV
Working distance	: 6-10 mm
Spot size	: 2.0
Counting rate	: 1-2 kcps
Detector type	: LFD
Cone	: X-ray
Signal	: Secondary electron

A low vacuum mode was applied whereby in these modes the column is under high vacuum and the sample chamber is at high pressure range of 130 Pa.

3.3.4 Thermogravimetric Analysis (TGA) and Differential Scanning Calorimetric analysis (DSC)

IUPAC definition of ‘thermal analysis’ is, ‘a variety of techniques in which a property of a system is recorded as a function of temperature, while the system is driven by a controlled temperature program’ [102]. Generally, there are two chief methods of interest:

Thermogravimetric Analysis (TGA)

Differential Scanning Calorimetry (DSC)

- Thermal methods are important for characterizing solids, in terms of identify, purity and physicochemical form. The method of thermogravimetry is basically quantitative in nature in that the mass-change can be accurately determined. Most TGA curves display weight losses. Figure 3.13 shows the thermal analysis instrument for determination of thermal stability, kinetic studies, material characterization (fingerprint), simulation of industrial process and compositional studies.

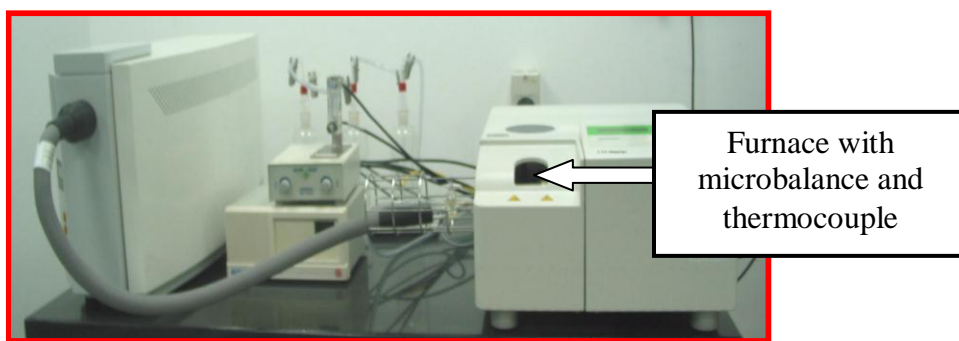


Figure 3.13: Thermal Gravimetric Analysis

TGA measures the mass of a sample (usually a few mg) as a function of its temperature while the temperature changes are according to a pre-planned program. It consists of a very sensitive balance (accurate to a few tenths of a microgram) for which the sample pan is suspended in a furnace. The furnace temperature can be controlled with an accuracy of about 0.1° and can be changed at rates of < 1 K/min or even higher. The mass is then plotted as a function of temperature and any lost material quantified and accounted for.

A common use of this technique is to quantify adsorbed moisture (non-stoichiometric) or crystal water (stoichiometric) besides testing the solid-state stability. In this case, the lost of mass may either be water (from chemical dehydration of the compound), or some other volatile material [103-104].

Another use for TGA is to estimate the intrinsic volatility of a compound, by measuring the rate of direct conversion from the solid phase to the gas phase (sublimation). Compounds with high internal energy tend to be more volatile than compounds with lower internal energy.

The main applications of thermogravimetry are summarized below:

Differential thermal analysis measures the transfer of heat energy (enthalpy, ΔH) to or from a sample as its temperature is raised or lowered in a small furnace [105]. If the sample maintains its form or structure while the temperature is changed, then the only property controlling the rate of temperature change is its heat capacity (ΔC_p). However, if the solid undergoes any sort of internal structural change, then its ΔC_p value changes substantially and the sample undergo a rapid change in heat flux (in or out) as shown on the differential scanning calorimeter (DSC) thermogram or scan by an exothermic or endothermic peak.

The DSC Mettler Toledo 822^e is used to perform the thermal analysis in this study as shown in Figure 3.14.



Figure 3.14: Differential Scanning Calorimeter for determination of melting points, phase change temperatures and chemical reaction temperature

The Nomenclature Committee of the International Confederation for Thermal Analysis (ICTA) has defined DSC as a technique in which the difference in heat flow (power) to the sample and to the reference material is monitored against time while the sample and reference material are subjected to a temperature program [106]. DSC therefore measures the amount of energy absorbed (endothermic event) or released (exothermic event) by a specimen either during continuous heating/cooling (dynamic or non-isothermal) experiments or during isothermal experiments (specimen maintained at a constant temperature).

The calibration is done by means of a standard (high purity indium) and can be measured with good accuracy. Likewise, the temperature at which the event occurs can be defined with an accuracy of about 0.1 ° [107, 108].

The types of internal structural change include the following:

- Melting points
- Polymorphic change
- Loss of surface moisture
- Loss of water of crystallization
- Sublimation (solid to gas vaporization)
- Chemical reaction

Experimental Conditions:

A Mettler Toledo TGA/SDTA 851^e unit, equipped with a microbalance and furnace with the heating facilities up to 1600 °C was used to investigate the thermal stability of Ti-MCM-41. The balance was purged with 50 cm³min⁻¹ of nitrogen as protective gas. The results were evaluated with the V7.01 STAR^e software package. The DTG curves are calculated as derivatives of the TGA curves. The SDTA curves were determined as the temperature difference between the measured sample temperature and the program temperature.

In this study, about 10-15 mg of Ti-MCM-41 samples were measured in an open alumina crucible of 70 µl volume at an elevated temperature from ambient to 800 °C at heating rate of 5 °Cmin⁻¹. Compressed air was used as reactive gas at a constant flow of 50 cm³ min⁻¹.

The DSC analysis was performed using Mettler Toledo DSC 822^e equipment with an intra-cooler. The DSC was calibrated (temperature and heat-flux) by melting Indium. In this analysis, similar amount of samples as for TGA (10-15 mg) was measured in a hermetically sealed 40 μ l alumina crucible, with a pierced hole of approximately 50 μ m in the lid of the crucible. Purge gas used was nitrogen at 50 $\text{cm}^3\text{min}^{-1}$. The DSC temperature program runs dynamically from ambient temperature to 700 $^{\circ}\text{C}$ at a heating rate of 5 $^{\circ}\text{Cmin}^{-1}$ under a constant air flow of 50 $\text{cm}^3\text{min}^{-1}$. The results were evaluated with the V7.01 STAR^e software package.

3.3.5 Ultraviolet Visible (UV-Vis) Absorption Spectroscopy

The diffuse reflectance UV-Vis spectroscopy (UV = 200–400 nm, visible = 400–800 nm) is known to be a very sensitive and suitable technique for studying electronic transitions. The adsorption of UV or visible radiation corresponds to the excitation of outer electrons. It is also useful for identification and characterization of metal ion coordination and its existence in the framework or extra-framework position of metal containing molecular sieves.

The position of “ligand-to-metal charge transfer” (L→M) band depends on the ligand field symmetry surrounding the metal center and the electronic transitions from ligand-to-metal require higher energy for a tetra-coordinated metal ion than for a hexa-coordinated one. For most of the isomorphously substituted

microporous and mesoporous metallo-silicate (particularly Ti- and V-containing) molecular sieves, transitions in the UV region (200-400 nm) are of prime interest.

There are three types of electronic transitions;

- transitions involving π , σ and n electrons
- transitions involving charge-transfer of electrons
- transitions involving d and f electrons

All possible transitions are shown in Figure 3.15.

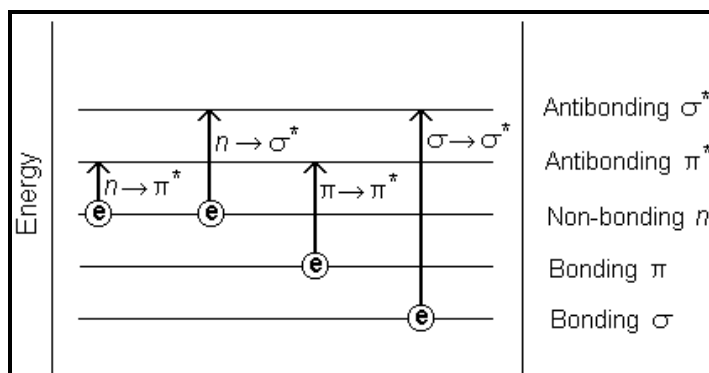


Figure 3.15: Possible electronic transitions of π , σ and n electrons [109].

When a sample is irradiated with UV light, the sample can absorb photons of energy which cause transitions between electronic energy levels. Normally, this is associated with transitions between bonding or lone pairs of electrons into non or anti bonding orbitals.

Figure 3.16 explains the radiation reflected from a powdered surface *e.g.* Ti-MCM-41 which consists of two components, *i.e.*;

- (i) that reflected from the surface without any transmission
- (ii) that adsorbed into the material and which then reappears at the surface after multiple scattering

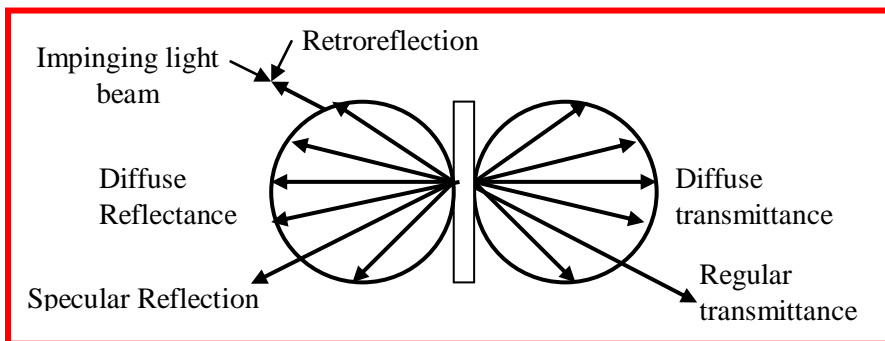


Figure 3.16: Interaction of powder sample with light

The latter is one that measured as reflectance in the DR-UV-Vis spectrum. The earlier reflection has no electronic interaction with the sample (no electronic energy absorption, merely mirror reflection). Since only small part of the diffuse radiation is returned to the detector, measurement of the diffuse intensity is difficult. For this purpose, a special integrating sphere, coated inside with a highly reflecting layer, such as MgO or Ba₂SO₄, is used. The sphere increases the part of the diffused intensity that reaches the detector (30-50%). The spectrums are recorded in ratio with a reference sample which has similar diffusion characteristic to the sample analyze, but without an absorption losses.

Diffuse reflectance data are often converted to absorptivities by the Kubelka-Munk function [110].

The utility of the function are explained below;

- (i) that it is proportional to concentration in certain idealized cases, most notably situations in which the scattering characteristics of all the samples are the same
- (ii) that data can be linearized with the function, making it available to be analyzed by chemometrics means.

To calculate the function, the measurable reflectance, R' can be used as follows:

$$F(R') = (1-R')^2 / 2 R' = \alpha / s$$

This quantity, for a layer of infinite thickness with α = absorptivity in units cm^{-1} and s = scattering factor (largely independent of wavelength for particle sizes larger than the light wavelength).

Experimental Conditions:

Diffuse Reflectance UV-Vis spectra were recorded using a Cary5G Spectrometer equipped with a reflectance attachment, an integrating sphere and a lamp change at 350 nm. All spectroscopic measurements were carried out over the range of 190-800 nm with a scan speed of 99.96 nm/min, and a nominal slit width of 1.00 nm. Ba_2SO_4 was used as reference in the measurements.

3.3.6 Fourier Transform Infrared Spectroscopy (FTIR)

Infrared Spectroscopy is the study of the interaction of electromagnetic radiation (infrared light) with a chemical substance. The nature of the interaction depends upon the properties of the substance. When radiation passes through a sample (solid, liquid or gas), certain frequencies of the radiation are absorbed by the molecules of the substance leading to the molecular vibrations. The frequencies of absorbed radiation are unique for each molecule, which provide the characteristics of a substance. The electromagnetic spectrum covers an immense range of wavelengths. The infrared regions are classified as follows:

- (i) Near Infrared 12500 to 4000 cm^{-1} (0.8 to 2.5 μm)
- (ii) Mid Infrared 4000 to 200 cm^{-1} (2.5 to 50 μm)
- (iii) Far Infrared 200 to 12.5 cm^{-1} (50 to 800 μm)

The functional group region (4000-1500 cm^{-1}) – Peaks in this region are characteristic of specific kinds of bonds, and therefore can be used to identify whether a specific functional group is present. The fingerprints region (1500-400 cm^{-1}) – peaks in this region arise from complex deformations of the molecule. They may be characteristic of molecular symmetry or combination bands arising from multiple bonds deforming simultaneously.

Any absorption band can be characterized by two parameters: the wavelength at which maximum absorption occurs and the intensity of absorption at this

wavelength. In an absorption spectrum, the y-axis measures the intensity of the band, which is proportional to the number of molecules observed. This principle consequently leads to quantitative analysis. Intensity of IR absorption is illustrated as below:

$$\text{Transmittance } T = I / I_0$$

$$\text{Absorbance } A = \log(1/T) = \log(I_0/I) = ECL$$

Where

I_0 = Intensity of incident radiation

I = Intensity of transmitted radiation

E = molar extinction coefficient

C = concentration (mole/l)

L = sample pathlength (cm)

FTIR spectroscopy is certainly one of the most important analytical techniques today. One of its great advantages is that any sample in any state can be studied: gas, liquids, solution, powders, films and surfaces can be examined by a suitable choice of sampling technique [111, 112].

The energy at which any peak in an absorption or transmission of FTIR spectrum appears corresponds to the frequency of vibration of a part of the sample molecule. This provides information on the functional groups in the molecule. From the frequencies of the absorption, it is possible to determine whether various functional groups are present or absent. This forms basis of analyses of the molecular structure of single and multi component materials [113]. The

movements of the atoms of a molecule during vibration can be classified as bond or angle deformations.

FTIR spectroscopy was carried out to determine the molecular functional groups embedded in the catalyst. FTIR is also an important method of structure characterization giving information on short range and long range bond order caused by lattice coupling and electrostatic and other effects. The characteristic group frequencies corresponding to the citric acid molecule were used to determine whether the catalyst kept its properties after heterogenization and during all the steps of the catalytic procedures.

Experimental Conditions:

Infrared spectra (FTIR) spectrum was recorded by means of a Bruker spectrometer (IFS66V/S) in the absorbance mode. As sample is optically too dense to measure the transmission spectral directly, catalyst was crushed into very small particles and was compressed into a KBr pellets at 20000 psi. Its surface was carefully flattened in order to increase the intensity of the IR beam by reflection. An FTIR spectrum was recorded in the absorbance mode. For all spectra recorded, a 32 scan data accumulation in a range 400-4000 cm^{-1} was carried out at a resolution of 4.0 cm^{-1} .